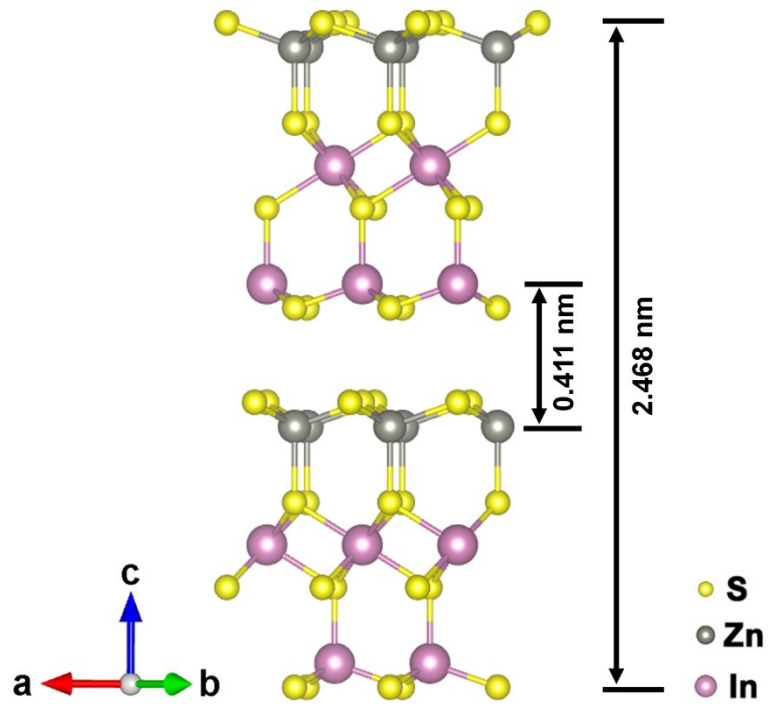


Supporting information

**Inert Basal Plane Activation of Two-Dimensional  
 $ZnIn_2S_4$  via Ni Atom Doping for Enhanced Co-  
catalyst Free Photocatalytic Hydrogen Evolution**

Xiaowei Shi,<sup>\*</sup> Liang Mao, Chao Dai, Ping Yang, Junying Zhang, Fuyuan Dong, Lingxia  
Zheng, Mamoru Fujitsuka,<sup>\*</sup> and Huajun Zheng<sup>\*</sup>



**Fig. S1** Crystal structure of hexagonal  $\text{ZnIn}_2\text{S}_4$ .

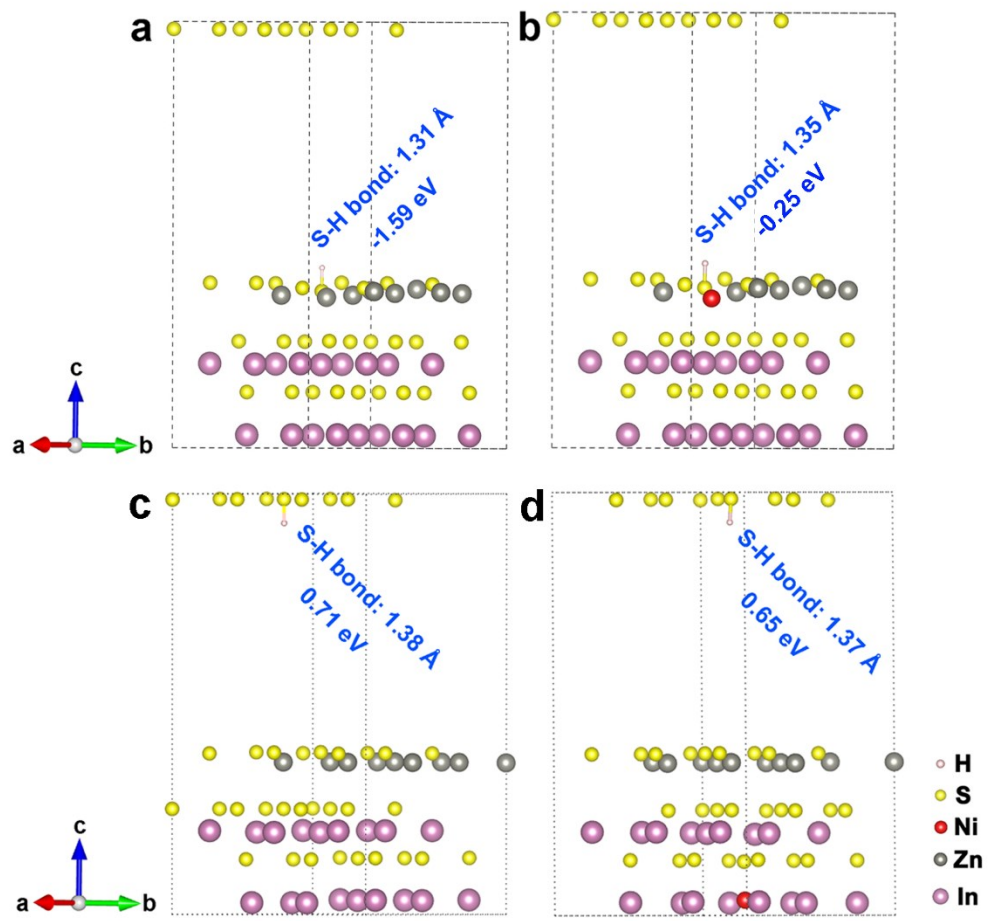


**Fig. S2** Bond length of S-H and corresponding  $\Delta G_H^*$  before (a) and after (b) Ni atom replacing Zn atom. Bond length of S-H and corresponding  $\Delta G_H^*$  before (c) and after (d) Ni atom replacing In atom.

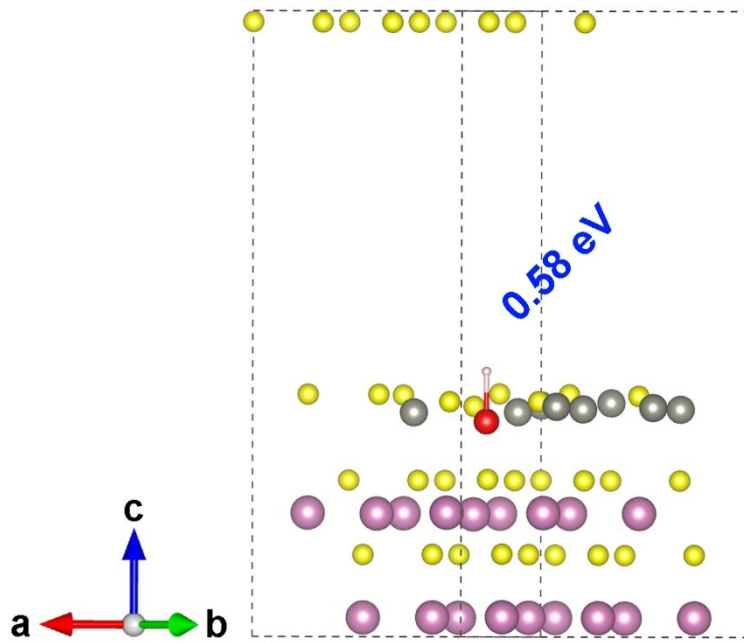


**Fig. S3** Calculated  $\Delta G_H^*$  at Ni atom in Ni-ZIS.

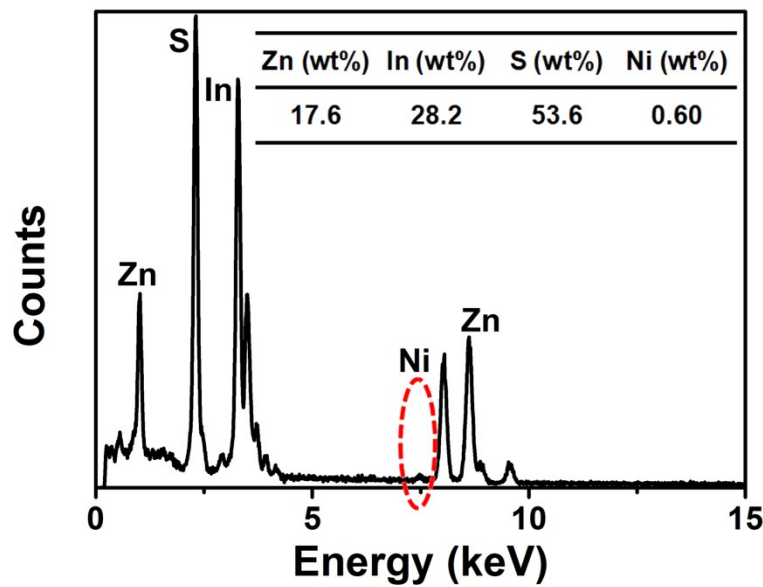


**Fig. S4** EDX pattern of  $\text{Ni}_{0.7}\text{-ZIS}$ .

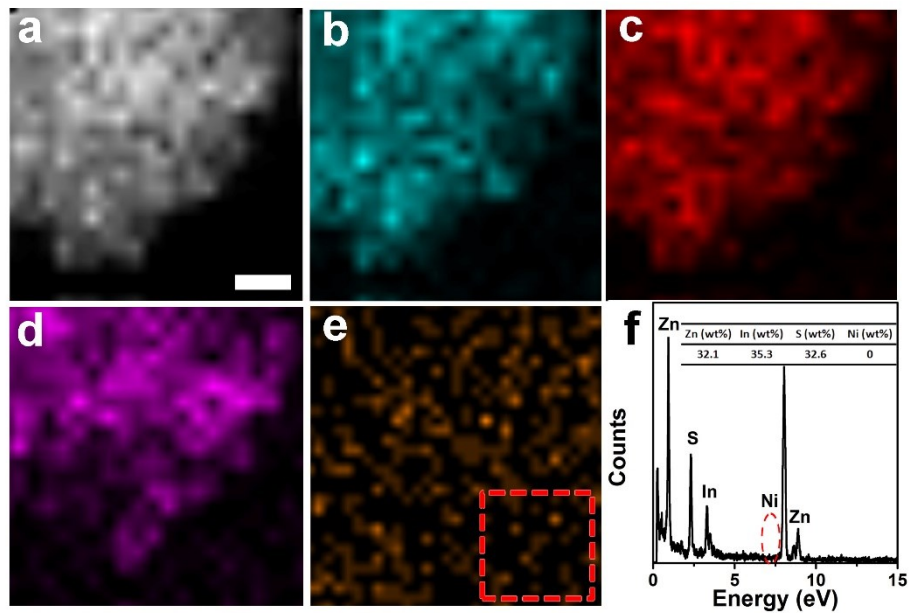


**Fig. S5** TEM (a) and elemental mappings of ZIS for Zn (b), S (c) and In (d), the corresponding scale bars are 100 nm. (f) EDX pattern of ZIS

Even though Ni signal is recorded, Ni peak could not be observed in the EDX pattern. More importantly, Ni signal is homogeneously distributed and it is detected even in the place where there is no ZIS nanosheets (red rectangular in Fig. S5e). Therefore, we suppose that the observed Ni signal may be caused by the noise rather Ni element.

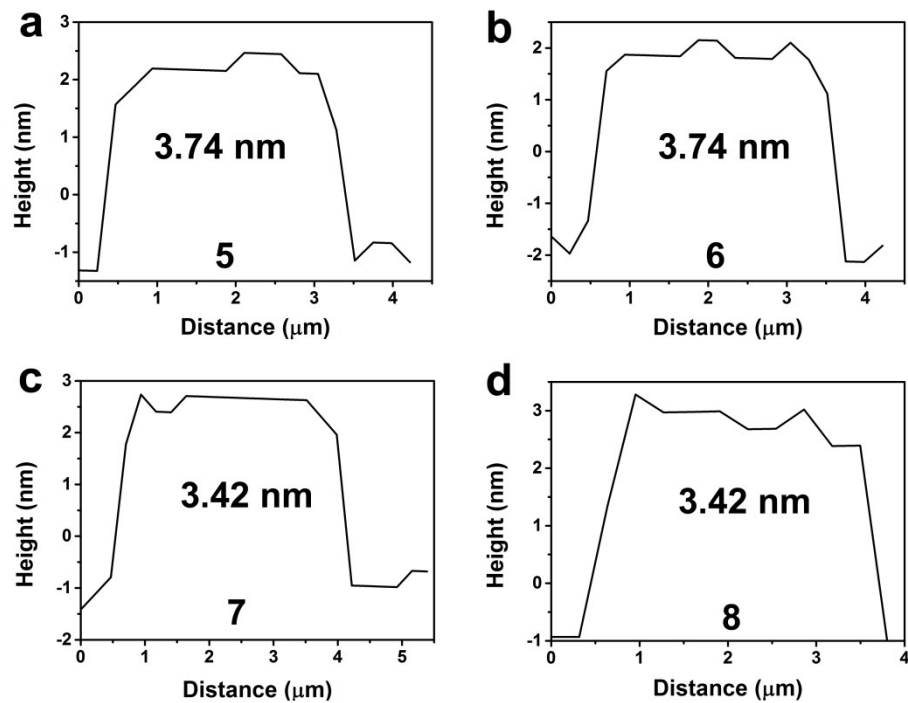


**Fig. S6** The corresponding height profiles of  $\text{Ni}_{0.7}\text{-ZIS}$  in Fig. 2g.

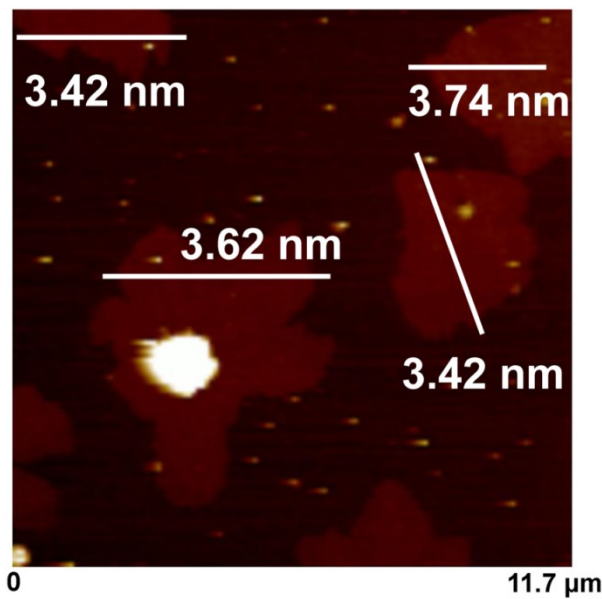


**Fig. S7** AFM image and corresponding height profiles of ZIS.

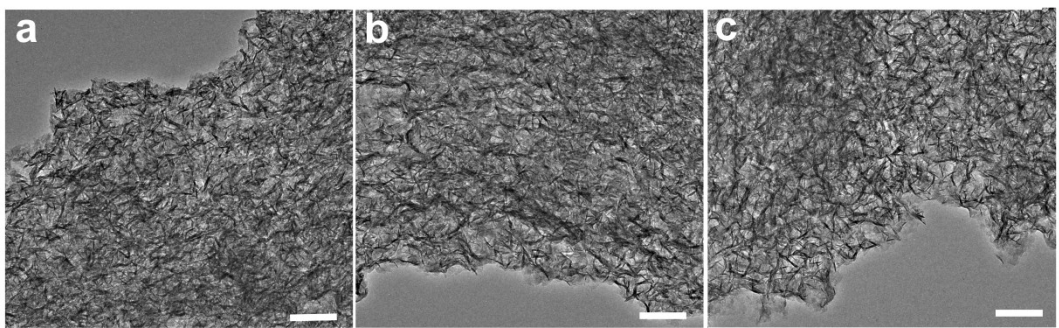


**Fig. S8** Morphology of  $\text{Ni}_{0.3}\text{-ZIS}$  (a),  $\text{Ni}_{1.4}\text{-ZIS}$  (b), and  $\text{Ni}_{2.1}\text{-ZIS}$  (c), the scale bar is 100 nm.

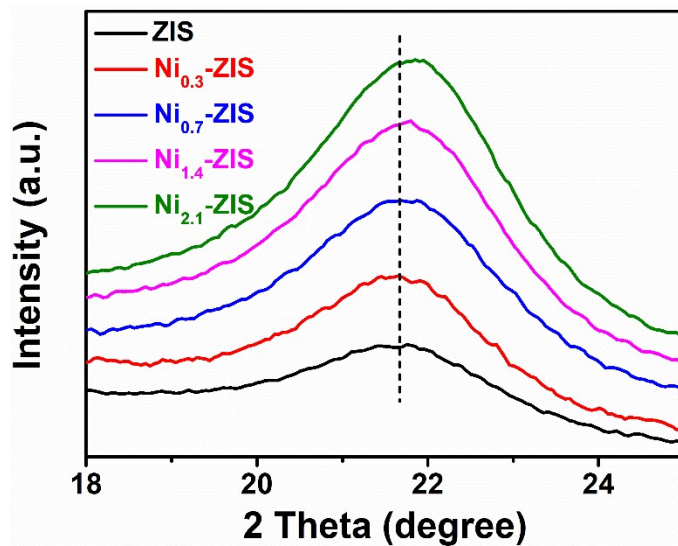


**Fig. S9** Enlarged XRD pattern of (006) peak for ZIS and Ni<sub>x</sub>-ZIS.

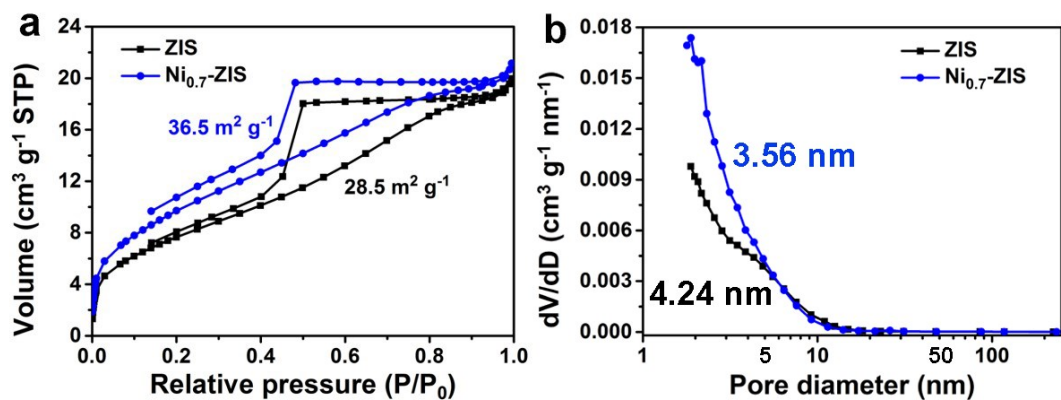


**Fig. S10** (a) Nitrogen adsorption/desorption isotherms of ZIS and Ni<sub>0.7</sub>-ZIS. (b) Pore diameter distribution of ZIS and Ni<sub>0.7</sub>-ZIS.

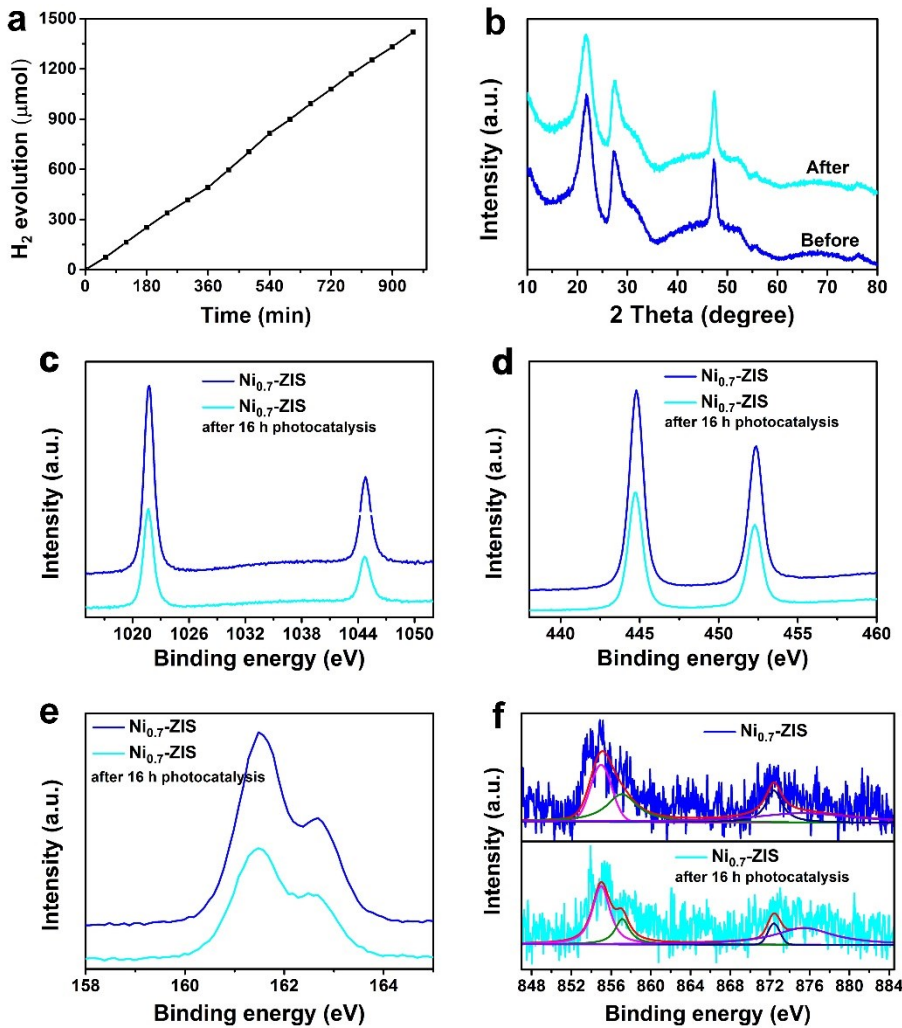


**Fig. S11** (a) Photocatalytic activity  $H_2$  evolution of  $Ni_{0.7}\text{-ZIS}$  for 16 h under visible light irradiation. (b) XRD patterns of  $Ni_{0.7}\text{-ZIS}$  before and after 16 h irradiation. High-resolution XPS results: Zn 2p (c), In 3d (d), S 2p (e) and Ni 2p (f) of  $Ni_{0.7}\text{-ZIS}$  before and after photocatalysis for 16 h.

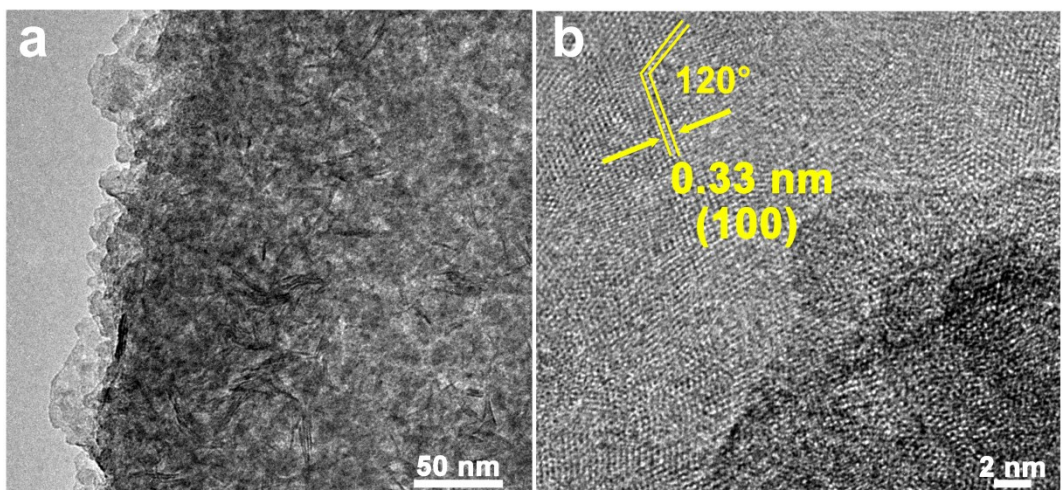


**Fig. S12** TEM (a) and HRTEM (b) images of  $\text{Ni}_{0.7}\text{-ZIS}$  after 16 h irradiation under visible light irradiation.

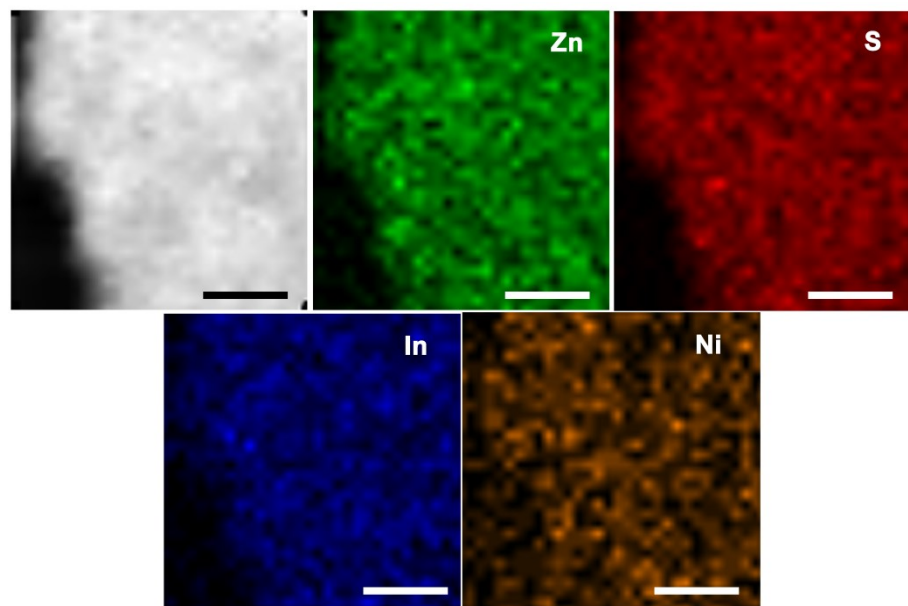


**Fig. S13** TEM and elemental mappings for Zn, S, In, and Ni in  $\text{Ni}_{0.7}\text{-ZIS}$  after 16 h visible light irradiation, the corresponding scale bars are 100 nm.

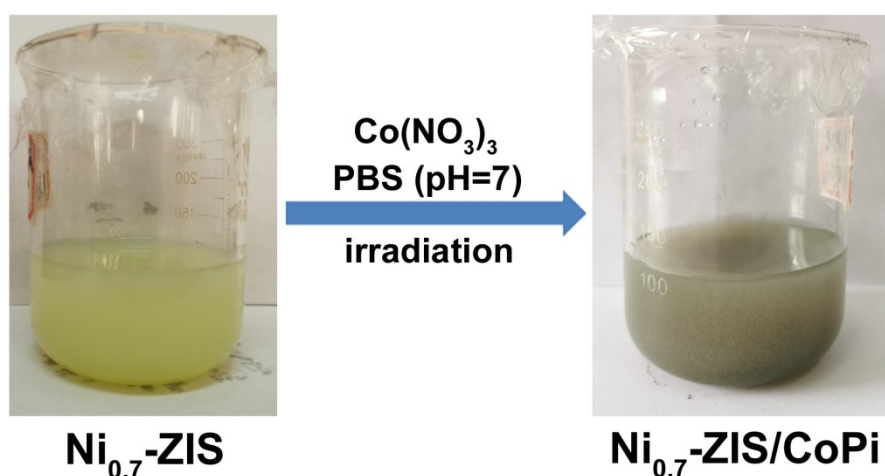


**Fig. S14** Photographs of Ni<sub>0.7</sub>-ZIS before and after photodeposition of CoPi.

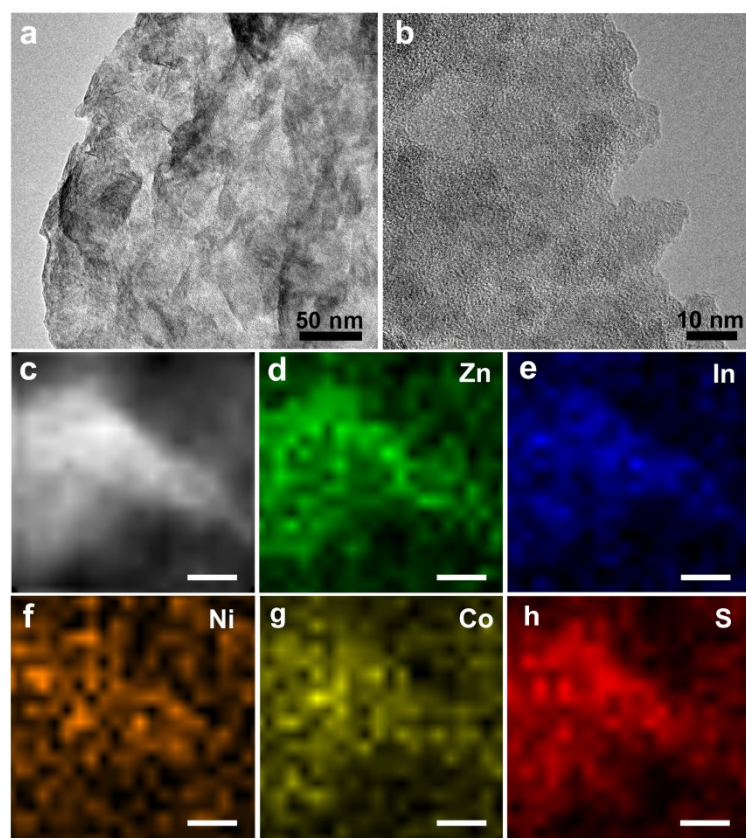


**Fig. S15** TEM (a) and HRTEM (b) Ni<sub>0.7</sub>-ZIS/CoPi. (c-h) TEM and elemental mappings for Zn, In, Ni, Co, and S in Ni<sub>0.7</sub>-ZIS/CoPi, the corresponding scale bars are 100 nm.

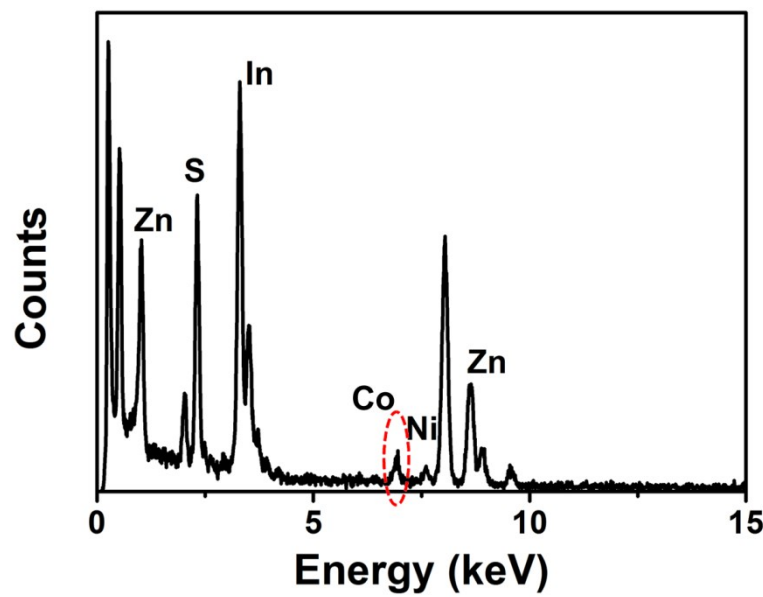


**Fig. S16** EDX pattern of  $\text{Ni}_{0.7}\text{-ZIS/CoPi}$ .

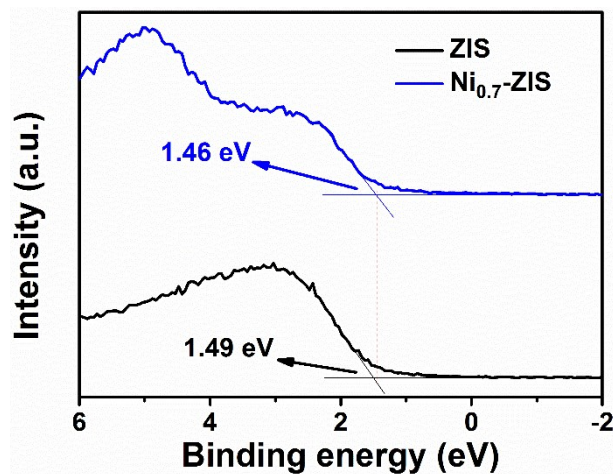


**Fig. S17** XPS valence band spectra of ZIS and  $\text{Ni}_{0.7}\text{-ZIS}$ .

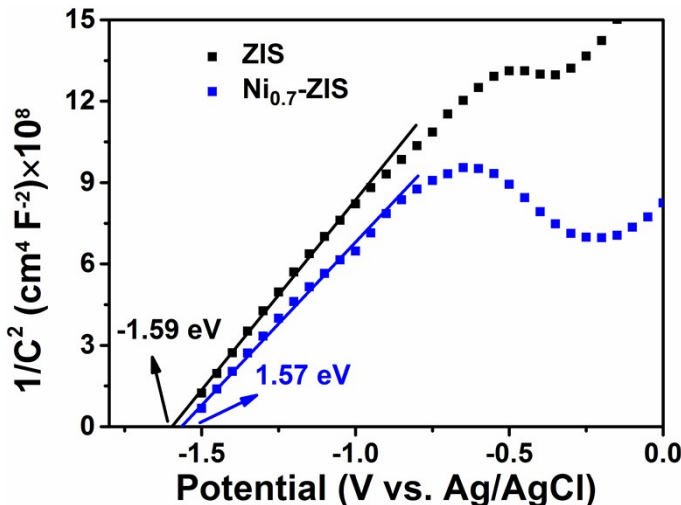


**Fig. S18** Mott-Schottky curves of ZIS and  $\text{Ni}_{0.7}\text{-ZIS}$ .

To acquire quantitative insight about the charge carrier density of ZIS and  $\text{Ni}_{0.7}\text{-ZIS}$ , the capacitance measurement on the electrode/electrolyte is conducted following the equation<sup>1</sup>:

$$\frac{1}{C^2} = \frac{2}{N_d e \epsilon_0 \epsilon} [(E_s - E_{fb}) - \frac{kT}{e}]$$

Where C is the space charge capacitance in the semiconductor,  $N_d$  is the electron carrier density, e is the elemental charge value,  $\epsilon_0$  is the permittivity of the vacuum,  $\epsilon$  is the relative permittivity of the semiconductor,  $E_s$  is the applied potential,  $E_{fb}$  is the flat band potential, T is the temperature and k is the Boltzmann constant.

The carrier density  $N_d$  can be determined using the following equation:

$$N_d = - \left( \frac{2}{e \epsilon_0 \epsilon} \right) \left[ \frac{d(E_s)}{d\left(\frac{1}{C^2}\right)} \right]$$

where  $e = 1.6 \times 10^{-19} \text{ C}$ ,  $\epsilon_0 = 8.86 \times 10^{-12} \text{ F m}^{-1}$ ,  $\epsilon = 4.7$ .<sup>2</sup> The calculated carrier densities of ZIS and  $\text{Ni}_{0.7}\text{-ZIS}$  are  $2.129 \times 10^{20}$  and  $2.443 \times 10^{20} \text{ cm}^{-3}$ , respectively, which are

almost the same.

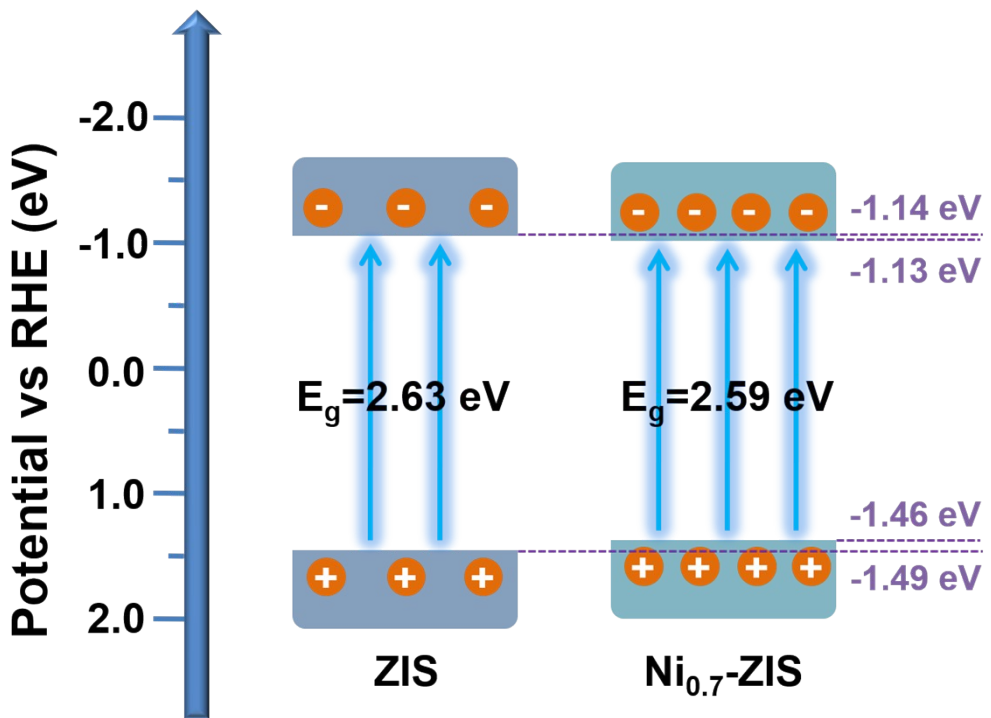


**Fig. S19** Schematic illustration of the band structure of ZIS and  $\text{Ni}_{0.7}\text{-ZIS}$  samples.

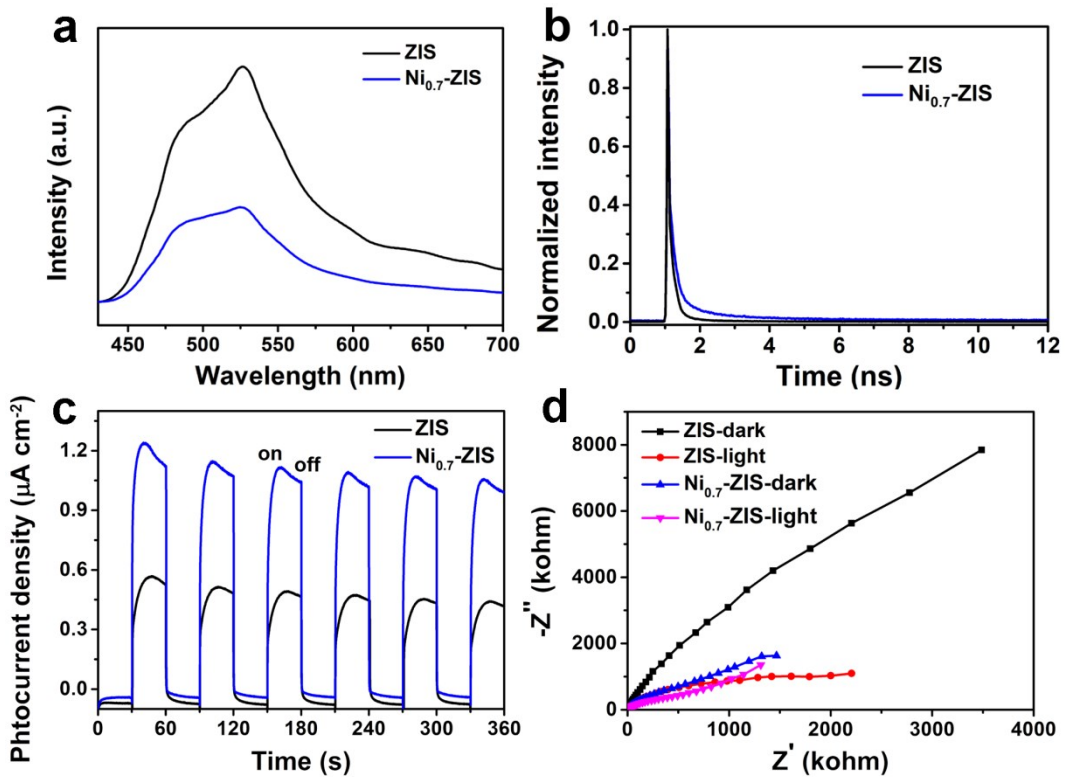


**Fig. S20** (a) Steady-state PL spectra of ZIS and Ni<sub>0.7</sub>-ZIS. (b) Time-resolved transient PL decay of ZIS and Ni<sub>0.7</sub>-ZIS. (c) Transient photocurrent responses of ZIS and Ni<sub>0.7</sub>-ZIS. (d) electrochemical impedance spectroscopy of ZIS and Ni<sub>0.7</sub>-ZIS under dark and visible light irradiation.

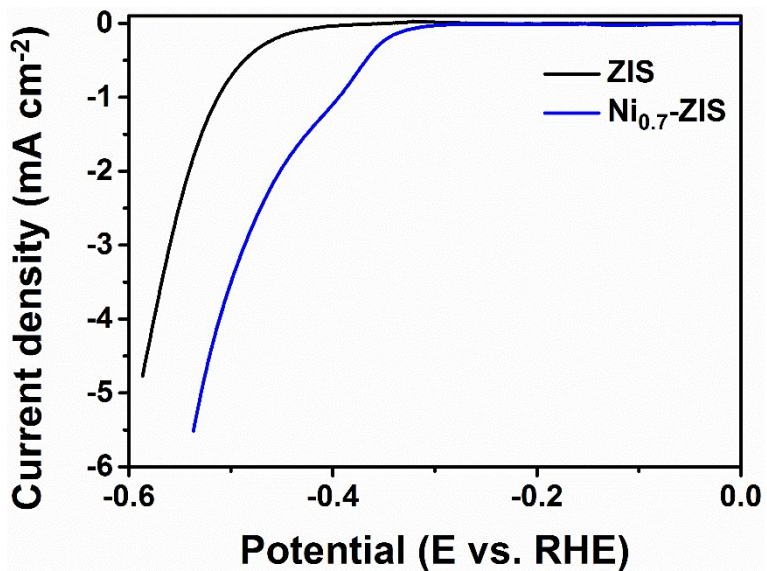


**Fig. S21** J-V curves of ZIS and Ni<sub>0.7</sub>-ZIS in 0.1 M NaOH aqueous solution without light irradiation.

**Table S1.** The different contents in ZIS and Ni-ZIS measured by ICP-MS and theoretical calculation.

Sample	Ni(NO <sub>3</sub> )·6H <sub>2</sub> O (mL)	Ni (wt%) ICP-MS	Ni (wt%) theoretical
<b>ZIS</b>	0	0	0
<b>Ni<sub>0.3</sub>-ZIS</b>	0.11	0.26	0.31
<b>Ni<sub>0.7</sub>-ZIS</b>	0.25	0.67	0.69
<b>Ni<sub>1.4</sub>-ZIS</b>	0.5	1.25	1.39
<b>Ni<sub>2.1</sub>-ZIS</b>	0.75	1.96	2.09

**Table S2.** H<sub>2</sub> evolution at each wavelength of Ni<sub>0.7</sub>-ZIS.

Wavelength (nm)	H <sub>2</sub> evolution (μmol)	Light intensity (mW·cm <sup>-2</sup> )
380	63.6	2
420	61.2	2
450	44.8	3
500	19.7	4.5
550	1.87	8
600	1.27	10
700	0	12

**Table S3.** Comparison of representative co-catalyst free photocatalysts and their H<sub>2</sub> evolution behaviors.

Catalysts	Sacrificial agent	H <sub>2</sub> (mmol g <sup>-1</sup> h <sup>-1</sup> )	AQE
Ni <sub>0.7</sub> -ZIS (this work)	TEOA (10 vol%)	4.215	17.1% (420 nm)
Ni <sub>0.7</sub> -ZIS (this work) (AM 1.5 G)	-	0.237	-
ZnIn <sub>2</sub> -Au-TiO <sub>2</sub> <sup>3</sup>	-	0.186	-
g-C <sub>3</sub> N <sub>4</sub> /nanocarbon/ZnIn <sub>2</sub> S <sub>4</sub> <sup>4</sup>	CH <sub>3</sub> OH (6 vol%)	0.05	-
2D/2D phosphorene/g-C <sub>3</sub> N <sub>4</sub> <sup>5</sup>	Lactic Acid (18 vol%)	0.571	1.2% (420 nm)
Black phosphorous/g-C <sub>3</sub> N <sub>4</sub> <sup>6</sup>	Methanol	0.427	3.18% (420 nm)
2D black phosphorus/BiVO <sub>4</sub> <sup>7</sup>	-	0.27	0.89% (420 nm)
Janus-like g-MnS/Cu <sub>7</sub> S <sub>4</sub> <sup>8</sup> (full-spectrum irradiation)	Na <sub>2</sub> S (0.35 M)/ Na <sub>2</sub> SO <sub>3</sub> (0.25 M)	0.718	18.8% (420 nm)
O-doped ZnIn <sub>2</sub> S <sub>4</sub> <sup>9</sup>	Na <sub>2</sub> S (0.35 M)/ Na <sub>2</sub> SO <sub>3</sub> (0.25 M)	2.12	-
Li-EDA treated P-25 <sup>10</sup> (AM 1.5 G)	Methanol (50 vol%)	3.46	2.57% (420 nm)
ZnIn <sub>2</sub> S <sub>4</sub> /g-C <sub>3</sub> N <sub>4</sub> <sup>11</sup>	TEOA (10 vol%)	2.6408	4.4% (420 nm)
DCN-200 <sup>12</sup>	TEOA (10 vol%)	0.135	-
Cu <sub>0.5</sub> -ZIS <sup>13</sup> (AM 1.5 G)	Asorbic acid (20% 0.75 M)	1.875	-
In <sub>2</sub> O <sub>3</sub> -ZnIn <sub>2</sub> Se <sub>4</sub> <sup>14</sup>	Na <sub>2</sub> S (0.35 M)/ Na <sub>2</sub> SO <sub>3</sub> (0.25 M)	0.32	-
In <sub>2</sub> O <sub>3</sub> -ZnIn <sub>2</sub> Se <sub>4</sub> -Mo <sup>14</sup>	Na <sub>2</sub> S (0.35 M)/ Na <sub>2</sub> SO <sub>3</sub> (0.25 M)	6.95	-

## Notes and references

- 1 Z. Zhang, Y. Yu and P. Wang, *ACS Appl. Mater. Interfaces* 2012, **4**, 990-996.
- 2 B. Assaker, M. Gannouni, A. Lamouchi and R. Chtourou, *Superlattices Microstruct.* 2014, **75**, 159-170.
- 3 G. Yang, H. Ding, D. Chen, J. Feng, Q. Hao and Y. Zhu, *Appl. Catal. B: Environ.* 2018, **234**, 260-267.
- 4 F. Shi, L. Chen, M. Chen and D. Jiang, *Chem. Commun.* 2015, **51**, 17144-17147.
- 5 J. Ran, W. Guo, H. Wang, B. Zhu, J. Yu and S.-Z. Qiao, *Adv. Mater.* 2018, **30**, 1800128.
- 6 M. Zhu, S. Kim, L. Mao, M. Fujitsuka, J. Zhang, X. Wang and T. Majima, *J. Am. Chem. Soc.* 2017, **139**, 13234-13242.
- 7 M. Zhu, Z. Sun, M. Fujitsuka and T. Majima, *Angew. Chem. Int. Ed.* 2018, **57**, 2160-2164.
- 8 Q. Yuan, D. Liu, N. Zhang, W. Ye, H. Ju, L. Shi, R. Long, J. Zhu and Y. Xiong, *Angew. Chem. Int. Ed.* 2017, **56**, 4206-4210.
- 9 W. Yang, L. Zhang, J. Xie, X. Zhang, Q. Liu, T. Yao, S. Wei, Q. Zhang and Y. Xie, *Angew. Chem. Int. Ed.* 2016, **55**, 6716-6720.
- 10 K. Zhang, L. Wang, J. K. Kim, M. Ma, G. Veerappan, C.-L. Lee, K.-j. Kong, H. Lee and J. H. Park, *Energy Environ. Sci.* 2016, **9**, 499-503.
- 11 B. Lin, H. Li, H. An, W. Hao, J. Wei, Y. Dai, C. Ma and G. Yang, *Appl. Catal. B: Environ.* 2018, **220**, 542-552.
- 12 G. Liu, G. Zhao, W. Zhou, Y. Liu, H. Pang, H. Zhang, D. Hao, X. Meng, P. Li, T. Kako and J. Ye, *Adv. Funct. Mater.* 2016, **26**, 6822-6829.
- 13 P. Wang, Z. Shen, Y. Xia, H. Wang, L. Zheng, W. Xi and S. Zhan, *Adv. Funct. Mater.* 2019, **29**, 1807013.
- 14 Y. Chao, P. Zhou, N. Li, J. Lai, Y. Yang, Y. Zhang, Y. Tang, W. Yang, Y. Du, D. Su, Y. Tan and S. Guo, *Adv. Mater.* 2019, **31**, 1807226.